PERFORMANCE AND UPGRADE OF THE FAST BEAM CONDITION MONITOR AT CMS

M. Hempel, DESY, Zeuthen, Germany*
B. Pollack, Northwestern University, Evanston, Illinois†
A. Bell, H. M. Henschel, O. Karacheban, W. Lange, W. Lohmann, J. L. Leonard,
M. Penno, S. Schuwalow, R. Walsh, DESY, Zeuthen, Germany
Dominik Przyborowski, University of Science and Technology, Cracow, Poland
David Peter Stickland, Princeton University, Princeton, New Jersey, USA
P. Bartowy, A. E. Dabrowski, R. Loos, V. Ryjov, A. A. Zagozdzinska, CERN, Geneva, Switzerland
K. Afanaciev, NC PHEP BSU, Minsk, Belarus
On behalf of CMS Collaboration

Abstract

The Fast Beam Condition Monitor (BCM1F) is a diamond based particle detector inside CMS. It consisted of 8 single-crystal chemical vapor deposition (sCVD) diamond sensors on both ends of the interaction point, and was used for beam background and luminosity measurements. The system has been operated with an integrated luminosity of 30 fb^{-1}, corresponding to a particle fluence of $8.78 \cdot 10^{-13}$ cm^{-2} (24 GeV proton equivalent). To maintain the performance at a bunch spacing of 25 ns and at the enhanced luminosity after the LHC Long Shutdown LS1, an upgrade to the BCM1F is necessary. The upgraded system features 24 sensors with a two pad metallization, a very fast front-end ASIC built with 130 nm CMOS technology, and new back-end electronics. A prototype of the upgraded BCM1F was studied in the 5GeV electron beam at DESY. Measurements were done on the signal shape as function of time, the charge collection efficiency as a function of voltage, and the amplitude as a function of the position of the impact point of the beam electron on the sensor surface. The preliminary results of this test-beam experiment and the status of the newly upgraded BCM1F will be presented.

BCM1F DURING OPERATION

BCM1F is a particle counter with nanosecond time resolution based on single-crystal chemical vapor deposition (sCVD) diamonds. Due to the linear dependence between detection probability and luminosity as shown in Figure 1, it is possible to use BCM1F as a luminosity monitor as well as a background monitor [1, 2].

During the first LHC running period from 2008-2012 BCM1F delivered online background and luminosity measurements as feedback for the CMS and LHC operation [3,4]. Since the data acquisition for BCM1F is decoupled from the main CMS DAQ, it could measure luminosity even before physics data was taken.

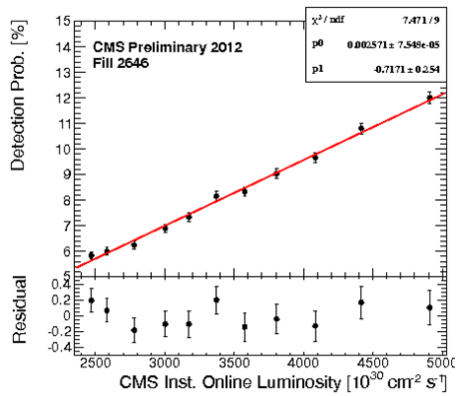

Figure 1: Particle detection probability as a function of luminosity.

MOTIVATION FOR THE BCM1F UPGRADE

The BCM1F modules are located around the beam pipe at a distance of 5 cm from the beam center. A particle fluence of $8.78 \cdot 10^{-13}$ cm^{-2} (24 GeV proton equivalent) at this position led to radiation damage of the laser diodes, which were used in the front-end electronics to convert the diamond sensor signal to an optical signal.

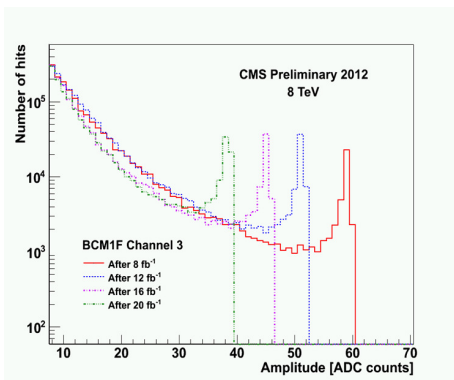

Figure 2: Decrease of the amplification measured by an ADC amplitude spectrum.

* maria.hempel@desy.de
† brian.lee.pollack@cern.ch

ISBN 978-3-95450-141-0

The observation of the amplitude spectrum measured by an Analog-to-Digital converter (ADC) showed a decrease in the amplification as a function of integrated luminosity, as illustrated in Figure 2. This decrease in amplification lead to inefficiencies because smaller signals could not be detected. Additional inefficiencies occurred due to very large signals in the sensors, as shown in Figure 3.

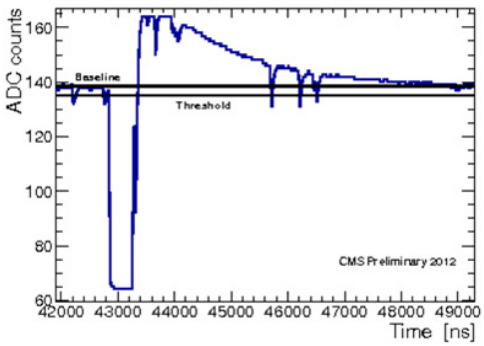

Figure 3: Amplitude as a function of time for large input signals.

These signals caused the front-end electronics to saturate for around 100 ns and signals could not be detected during this time. After the saturation, the amplitude shows an overshoot for a few μs. All signals that arrived during this time are detected with less efficiency.
Additionally, the proton bunch spacing for the future LHC run will be 25 ns, comparable to the peaking time of the amplifier. This potentially leads to pile-up of subsequent signals.

BCM1F FRONT-END UPGRADE

All BCM1F components are upgraded in order to match the demanding requirements corresponding to higher luminosity and smaller (25 ns) bunch spacing.

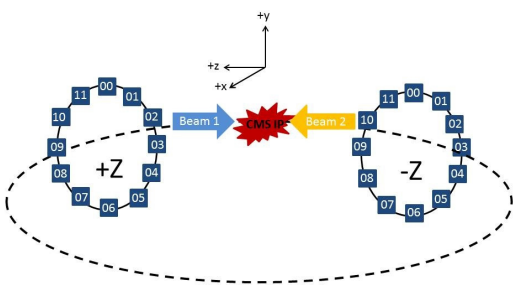

Figure 4: Upgraded BCM1F layout with 12, 2-pad sCVD sensors on each side of the CMS interaction point. Distance between the CMS interaction point and sensors is 1.8 m

Firstly, the number of sensors is increased from 8 to 24 sCVD in order to improve the acceptance of the background measurements. The new BCM1F layout is illustrated in Figure 4 and contains 12 sensors on each side of the interaction point. The distance between the sensors and interaction point will be the same as in the first running period at 1.8 m. Each sensor has a two pad metallization as shown in Figure 5 in order to decrease the count rate. The width of the gap between the two pads is between 5 and 25 μm.

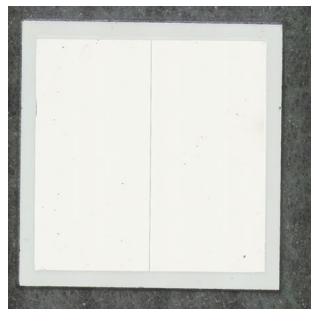

Figure 5: Two pad metallization of sCVD sensors.

A new dedicated front-end ASIC, developed at CERN in collaboration with the University of Science and Technology AGH Krakow, is based on 130 nm CMOS technology and includes a fast trans-impedance preamplifier with an active feedback, a shaper stage and a fully differential output buffer. A better charge-to-voltage conversion of 50 mV/fC is obtained (previously was 20 mV/fC). Measurements done in the laboratory show a FWHM of less than 10 ns as shown in Figure 6.

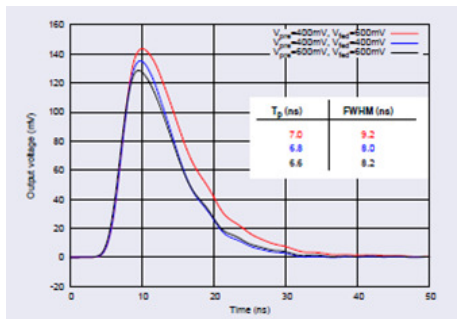

Figure 6: The ASIC output signal for various feedback and bias settings as a function of time for an injected test charge, which corresponds to one minimum ionizing particles.

In order to characterise the impact of overshoots, a very large signal was fed into the front-end ASIC and the response was measured. As can be seen in Figure 7, the amplitude shows fast baseline recovery after about 30 ns.

The upgraded carriage design, as shown in Figure 8, has two main parts: the C-shape, each of which holds 6 sensors and their corresponding front-end ASICs, and the flexible regions where the optical board will be placed. This design allows the placement of the analog opto-hybrid board (AOH) to be further away from the beam center (16 cm as opposed to 5 cm), which reduces the radiation load to the lasers.

A C-shape assembled with the electronic parts is shown in Figure 9. The six square gold pads will hold the sensors and supply the bias voltage.

ISBN 978-3-95450-141-0

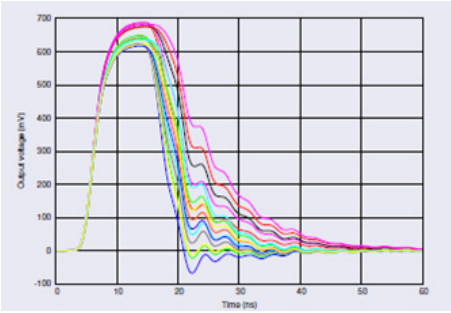

Figure 7: The ASIC output signal as a function of time for large (150 fC) injected input signals.

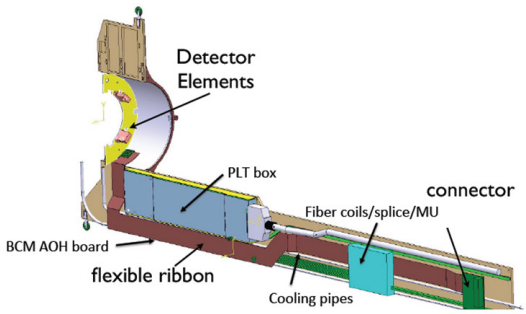

Figure 8: Upgraded carriage design with the C-shape and flexible parts that hold the sensors, front-end ASICs, and the optical board.

TESTS OF FRONT-END PARTS

Sensors and analog optical hybrid boards (AOHs) were characterised in the laboratory. The performance of a prototype detector, comprising of a sensor, front-end ASIC, AOH, and fast digitizer was measured in a test-beam.

Measurements in the Laboratory

The leakage currents were measured for the sensors as a function of bias voltage. A result is shown in Figure 10. The currents are in the pA range as expected, due to the very high band gap for diamonds 5.4 eV.

The charge collection efficiency (CCE), defined as the ratio between the measured charge and expected charge of the diamond at a given bias voltage, was measured. Figure 11 shows, as an example, the CCE as a function of bias voltage. A maximum CCE of around 95 % above 40 V was obtained.

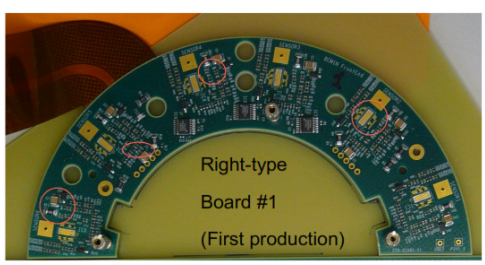

Figure 9: C-shape with mounted electronics.

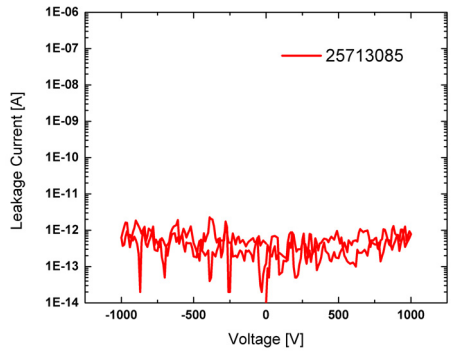

Figure 10: Measured leakage current as a function of bias voltage for an sCVD diamond sensor.

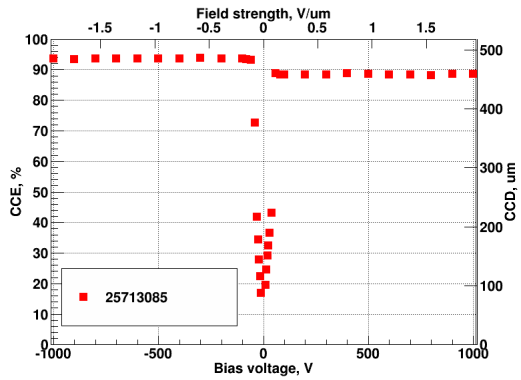

Figure 11: Measured CCE and charge collection distance (CCD) as a function of bias voltage for a sensor.

In order to determine the turn-on voltage and the linearity of the response of the laser, the output signal was measured as a function of the input voltage. The results are shown in Figure 12. Linearity up to 1.2 V input voltage is observed.

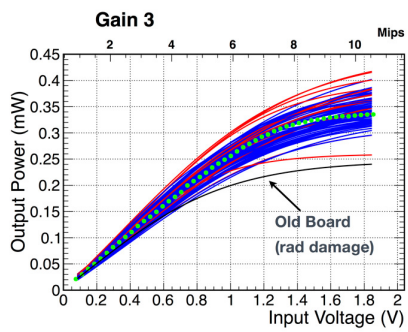

Figure 12: Response of the laser as a function of signal strength.

Test-Beam Results

The test-beam measurements were performed at DESY II using a 5 GeV electron beam at a rate of 100 Hz. The signals generated by the beam electrons were triggered by scintillators of 1 cm^2 effective area located before and after the

ISBN 978-3-95450-141-0

test setup, and 6 Mimosa26 telescope planes were used to reconstruct the tracks of triggered electrons. The full readout chain, consisting of sensor, the front-end ASIC, and AOH was characterised.

A signal, measured by a sampling ADC, is shown in Figure 13. The amplitude of this signal corresponds to a minimum ionizing particle in a sensor with 80 %CCE. The FWHM of the signal is less than 10 ns, matching the design requirements.

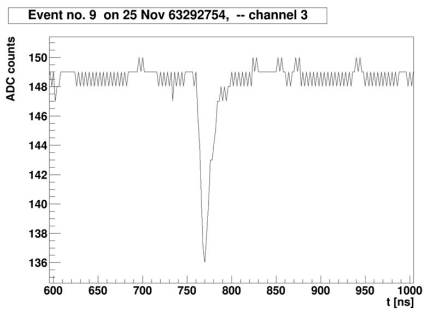

Figure 13: Signal from a triggered electron as a function of time.

A scan of the CCE as a function of the impact point of the electron beam was done to measure the uniformity of the response over the sensor surface. The result, shown in Figure 14, was a flat CCE of about 80 % over the metallised area. Charge sharing between the pads was observed in the region of the gap. However, the gap size was on the order of 5 μm, much less than the width of the charge sharing range.

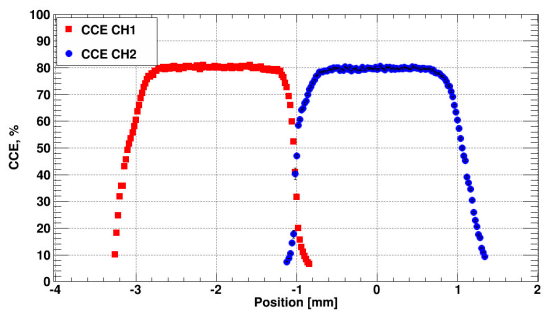

Figure 14: The CCE as a function of the position of the beam electron impact point.

An explanation of this observation is given by a simulation using the program called “Superfish” [5] that calculates the weighting potential of a sensor with two pads and a CCE of 80 %. The weighting potential, as discussed by Ramo [6] and H. Spieler [7], determines the coupling of a moving charge carrier at any position to an electrode.

The simulations were done setting the bottom pad of the sensor and the top right pad to 0 V, whereas the top left readout pad was set to 1 V, as illustrated in Figure 15. The uniform electrical field will force a free charge carrier to travel perpendicular to the read out pads.

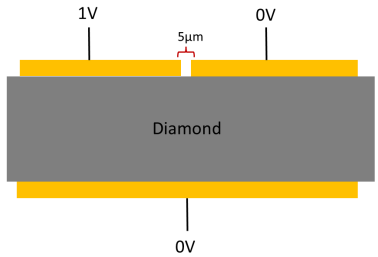

Figure 15: Sensor structure used in the Superfish simulations.

Figure 16 shows the comparison between the measurements of the left readout pad (red) and three different types of simulated weighting potentials. The green curve represents the prediction for a sensor that has a 20 % reduced CCE directly under the top pad. The magenta curve represents the prediction for a 20 % reduced CCE at the bottom pad, and the blue curve represents the due to a 10 % reduction at the top electrode and a 10 % reduction at the bottom electrode. The magenta curve does not agree with the measurements and thus that scenario can be excluded. The other two curves describe the test-beam results moderately well. It can be concluded that at least some of the inefficient sensor material is located close to the top readout pad.

SUMMARY

All components of the fast beam condition monitor, BCM1F, were upgraded, including the sensors, the front-end ASICs, and the mechanical structure. All front-end parts were tested in the laboratory and in a test-beam. The functionality of the full system was demonstrated and the relevant parameters match the requirements.

ISBN 978-3-95450-141-0

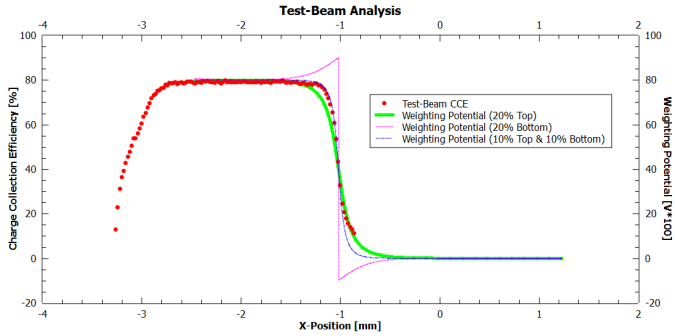

Figure 16: Comparison of the measurements and Superfish simulations of the charge sharing between the pads of a sensor with a charge collection efficiency of 80 %.

REFERENCES

[1] N. Odell, " Measurements of Luminosity and Normalised Beam-Induced Background Using the CMS Fast Beam Condition Monitor," Contribution to ICHEP2012, Melbourne, Australia, PoS(ICHEP2012)526

[2] A. Dabrowski, et al., " The Performance of the Beam Conditions and Radiation Monitoring System of CMS," Contribution to IEEE Nuclear Science Symposium and Medical Imaging Conference 2011, Valencia, Spain, CMS CR 2011/275

[3] A. J. Bell, " Fast Beam Conditions Monitor BCM1F for the CMS EXperiment," Nucl. Instrum. Methods Phys. Res., A 614 (2010) 433-438

[4] E. Castro, et al. " Application of Single Crystal Diamonds (scCVD) as Beam Coniditions Monitors at LHC," IBIC2012, Tsukuba, Japan, TUPA08

[5] R. F. Holsinger, et al. "SUPERFISH - A Computer Program for Evaluation of RF Cavities with Cylindrical Symmetry," Particle Accelerators 7 (1976) 213-222

[6] S. Ramo, "Currents Induced by Electron Motion," Proceedings of I.R.E. 27 (1939) 584-585
http://ieeexplore.ieee.org/stamp/stamp.jsp?tp=&arnumber=1686997

[7] H. Spieler, "Semiconductor Detector Physics," Oxford University Press 2005,
ISBN: 0-19-852784-5 978-0-19-852784-8

ISBN 978-3-95450-141-0